J Mater Sci: Mater Electron (2016) 27:7788–7794
DOI 10.1007/s10854-016-4767-z

CrossMark

The influence of Yttrium on leakage current and dielectric properties of amorphous Al_2O_3 thin film derived by sol–gel

Manwen Yao[1] · Pei Zou[1] · Zhen Su[1] · Jianwen Chen[1] · Xi Yao[1]

Received: 13 January 2016 / Accepted: 31 March 2016 / Published online: 21 April 2016
© Springer Science+Business Media New York 2016

Abstract Amorphous Yttrium-doped aluminum oxide thin films were deposited on Pt/Ti/SiO_2/Si substrates by sol–gel. It was observed by field emission scanning electron microscope that the surface morphology was smooth and homogeneous. From Fourier Transform Infrared Spectroscopy, a broad absorption band at 700–1000 cm^{-1} owing to vibrations of aluminum oxide was observed. The absorption peaks strength relating to hydroxyl group decreased with the increase of Y doping concentration. The electrical properties were investigated in terms of Y doping content and relative humidity. The results show that the existence of hydroxyl and absorbed water makes a significant influence on the electric properties of films. The electric conduction characteristics and dielectric breakdown properties are modified by the decrease of content of hydroxyl and absorbed water, leading to a lower leakage current and higher dielectric strength. It can be seen that the leakage current of films decreases with the Y doping, and could be reasonably deduced that leakage current can be effectively tuned by Y doping.

1 Introduction

Aluminum oxide is one of the most widely used materials with excellent characteristics of stable chemical and physical properties. In particular, aluminum oxide films have been important in both pure and applicative scientific research [1]. Over the past decade, aluminum oxide film has been used as a protective coating for its high resistance to radiation and corrosion [2, 3]. And owing to its outstanding insulating property, aluminum oxide film is also applied as insulator layers in electronic devices [4, 5]. Aluminum oxide film has accordingly received an increasing amount of interest and attention due to its widespread application [6, 7]. For instance, for its excellent insulating performance, aluminum oxide films have been being investigated as alternatives of gate oxides to SiO_2 on metal–oxide–semiconductor (MOS) based structures and relevant researches have been reported [8–11]. It is also indicated from simulations that Al_2O_3 deposited by sputtering is thermally stable and mechanically hard [12], which may be good for the gates of flash memory circuits. The reason is that Al_2O_3 with higher dielectric constant increases the capacitive coupling and circuit speed by three orders of magnitude, compared to SiO_2 [13]. Moreover, due to its high breakdown strength, aluminum oxide film is expected to be employed in solid state capacitors as one of the high energy storage dielectric materials. As many papers report, the relative permittivity and, more importantly, breakdown strength are the key parameters for energy storage dielectrics [14]. It is obviously seen that the improvement of energy storage density of dielectrics depends on the enhancement of relative permittivity and breakdown strength [15]. In addition, the reliability of electric devices is closely relative to leakage current and breakdown of dielectrics. Therefore, the relative permittivity, breakdown strength and leakage current are critical to the energy storage dielectrics. In the past years, many investigations have been carried out to study the high energy storage dielectrics and try the best to further improve the energy storage density [16, 17].

✉ Manwen Yao
yaomw@tongji.edu.cn

[1] Key Laboratory of Advanced Civil Engineering Materials, Ministry of Education, School of Materials Science and Engineering, Tongji University, No. 4800 Caoan Road, Shanghai 201804, China

Defect chemistry is the study of deviations from perfect order in inorganic compounds and effects of such disorder on their properties, including ionic conductivity and electronic conductivity. The presence of local deviations from perfect order can make a remarkable influence on the transport of mass or charge [18]. The generation of defects associated with doping usually acts as a two-edged sword in the aspect of dielectric properties of materials. The widely applied technology of doping, where atoms or ions of appropriate element are added to a basis material, is favorable to modify the materials to yield hybrid materials with desirable properties [19, 20]. So in our current work, we have been doing the research in order to study the leakage current and dielectric breakdown properties of aluminum oxide films by the doping technique.

To the best of our knowledge, the electric properties of Y-doped Al_2O_3 thin films deposited by sol–gel in MIM structures have not been reported till date. Therefore, the aim of this paper is to characterize Y-doped Al_2O_3 thin films prepared by sol–gel and evaluate their compositional tenability in terms of permittivity, leakage current and breakdown strength, which are important for the applications of energy storage dielectrics.

2 Experiment

For the preparation of aluminum oxide and Y doping sols, Aluminum isopropoxide ($Al(OC_3H_7)_3$) and Yttrium nitrate hexahydrate ($Y(NO_3)_3{\cdot}6H_2O$, 99 %), glacial acetic acid, glycol ether and acetylacetone, which were all of reagent-grade purity and available commercially, were used without further purification. Firstly, Aluminum isopropoxide and Yttrium nitrate hexahydrate were dissolved in glycol ether with continuous stirring for 30 min at 60 °C. Then, acetylacetone as chelating agent was added to the above solution and stirred for another 30 min. Lastly, the mixture solution with the addition of a certain amount of glacial acetic was heated to 80 °C, followed by stirring for 30 min. Subsequently, the mixture was cooled down to room temperature to obtain a clear, translucent, homogeneous and stable sol. The resultant sol was aged for 24 h and served as the coating sol. Platinized silicon ($Pt/Ti/SiO_2/Si$) wafers used as substrates were washed with acetone, ethanol and distilled water in an ultrasonic bath for 10 min, respectively, and then blow dried with N_2.

The coating sols were deposited on substrates by spin-coating at 3000 rmp for 20 s. To reach the desired thickness, spin-coating should be repeated many times. After each deposition, the films were preheated in a tubular furnace at 150, 300, 450 °C for 5 min respectively to obtain solid films. The target sol–gel films were annealed at 450 °C for 3 h in a muffle furnace.

The phase structure of films was identified by Grazing incident X-ray diffraction (GIXRD) on a Rigaku D/max-2550 X-ray diffractometer with Cu Kα radiation. The chemical composition of the films was characterized by Fourier Transform Infrared Spectroscopy (FTIR, Nicolet IN 10, USA). The surface morphology was observed by a field emission scanning electron microscopy (FESEM) (S-4700, HITACHI, Japan). The thickness of the films was measured by the cross-sectional FESEM images. For electrical measurements, samples were in the form of MIM structure parallel-plate capacitor with gold-plated circular electrodes as top electrode and Platinum as down electrode. Au electrode pads being 1 mm in diameter were sputtered by DC sputtering. Current–voltage was performed to measure leakage current and dielectric strength by using a Keithley 2400 electrometer connected to a computer with built-in self-programmed software. By using a voltage stress probe station, positive voltage was applied on the top electrode in a successive voltage step of 0.2 V with delay time of 0.1 s until the leakage current increased abruptly indicating the dielectric breakdown of the films. The dielectric properties were measured by using a Precision Impedance Analyzer Agilent E4980A LCR meter.

3 Results and discussion

3.1 Phase identification and morphology

$Al_{2-2x}Y_{2x}O_3$ films were deposited on $Pt/Ti/SiO_2/Si$ substrates by sol–gel described above in detail. According to the X-ray diffraction patterns of Al_2O_3 (AO), $Al_{1.96}Y_{0.04}O_3$ (AYO-2), $Al_{1.9}Y_{0.1}O_3$ (AYO-5) and $Al_{1.8}Y_{0.2}O_3$ (AYO-10), it indicates an amorphous phase independence of Y doping. As seen in Fig. 1a, the surface micrograph of undoped aluminum oxide films is selected to be shown in this paper. The micrograph shows a smooth and homogeneous surface, suggesting an amorphous structure. From the cross-section micrograph, the thickness of thin films is obtained and crystalline grains have not been found. It further verifies the amorphous structure independent of Y doping. The thickness of $Al_{2-2x}Y_{2x}O_3$ ($x = 0, 0.02, 0.05, 0.1$) films is 234, 234, 190, 201 nm, respectively.

3.2 FTIR spectra

Figure 2 shows the FTIR spectra of Y-doping aluminum oxide thin films. It can be observed that a broad absorption band located from 700 to 1000 cm^{-1}in spectra, which is typical of the vibrations of Al_2O_3. The absorption band consists of the contribution of the vibrations of aluminum oxide which change their shape, position and transition probability depending on the chemical form of the

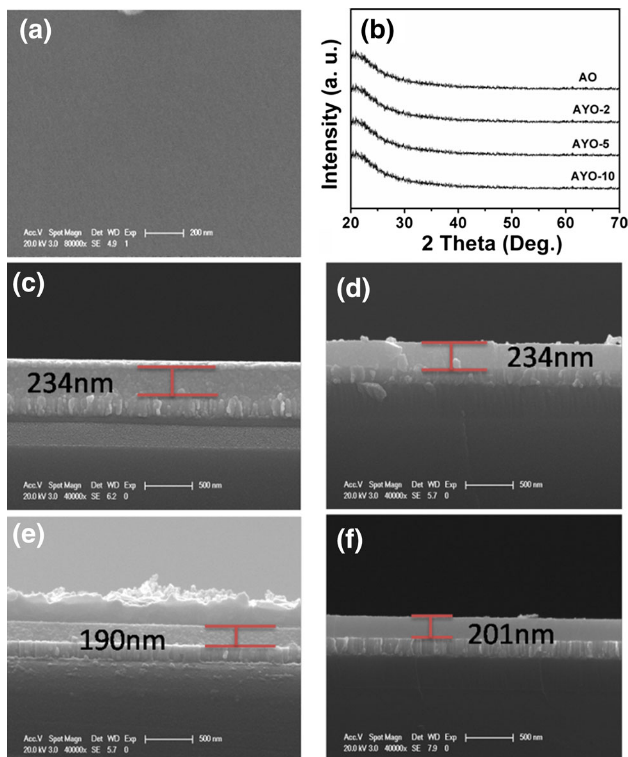

Fig. 1 Surface morphology of Al_2O_3 thin film (**a**); XRD patterns of $Al_{2-2x}Y_{2x}O_3$ thin films (**b**); cross-section FESEM micrographs of $Al_{2-2x}Y_{2x}O_3$ thin films (**c**—0 mol%, **d**—2 mol%, **e**—5 mol%, **f**—10 mol%)

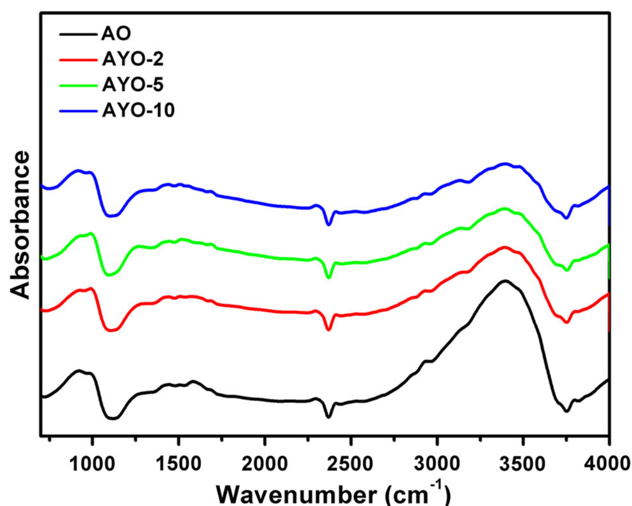

Fig. 2 FTIR spectra of $Al_{2-2x}Y_{2x}O_3$ thin films

aluminum oxidation [21]. The absorption peak at about 920 cm^{-1}should be attributed to LO mode peak, which is considered to be the combination of different phase (amorphous 959 cm^{-1}; γ-Al_2O_3 917 cm^{-1} [22]). This result turns out that the films may be the combination of amorphous and γ-Al_2O_3, despite the fact GIXRD indicates an amorphous structure. The explanation for the difference between FTIR and GIXRD may be that the γ-Al_2O_3 crystalline grain is in nanometer scale, which cannot be identified by GIXRD. And the phase structure of aluminum oxide is independent of Y doping.

It is important to remark that a broad absorption peak with a band center at 3400 cm^{-1} and a small shoulder around 3200 cm^{-1} are observed. The broad absorption at 3200–3470 cm^{-1} is related to Alanol groups (Al–OH) while the absorption peak centered around 1642 cm^{-1} is assigned to the bending mode of absorbed water. It should also be noted that there is a small absorption around 3800 cm^{-1}. It may be identified as isolated hydroxyl groups that become hydrogen-bonded to molecular water [23]. As Y doping content increases, there is a large decrease in intensity from 3000 to 3800 cm^{-1}. The results indicate that aluminum oxide films doped with Y have a relatively higher stability against water absorption than pure aluminum oxide films when kept at air atmosphere at room temperature.

3.3 Analysis of leakage current

Leakage current is crucial to the reliability of electric devices. Small leakage current is beneficial to the application of dielectrics. Figure 3 shows the current density versus electric field (*J–E*) characteristics of thin films. Current–voltage (I–V) measurements were tested in an test chamber maintaining ambient atmosphere at a temperature of 25 °C and relative humidity of 25 %. At low field region (0–140 MV/m), leakage current decreases with the increase of Y doping concentration. Leakage current density of AYO-10 is two orders of magnitude lower than the pure aluminum oxide films at 50 MV/m. Usually, ionic conductivity is small in the crystal structure, since the ionic

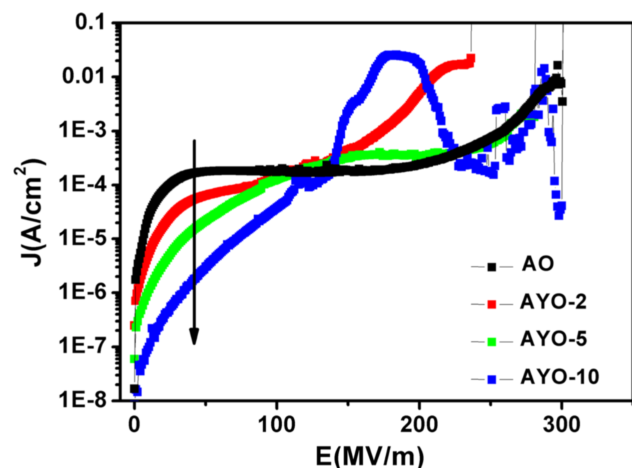

Fig. 3 The dependence of leakage current density on electric field for $Al_{2-2x}Y_{2x}O_3$ thin films based on MIM capacitors

mobilities are small. However, we cannot rule out the possibility of rapid diffusion which result from the amorphous or microcrystalline nature of insulator [24]. Thus, it is reasonable to deduce that ionic migration can be triggered under the electric filed in amorphous structure.

The decrease of leakage current at low field region can be attributed to the inhibition of ionic migration and the increase of defect associates with low mobility. On the one hand, the ionic radius of Y^{3+} (0.9) is larger than Al^{3+} (0.535). The difference of ionic radius leads to the local lattice defects which hinder the ionic migration and diffusion. On the other hand, the combination of two intrinsic ionic defects is referred to as a defect associate [18]. The bound vacancy associates have no net charge and do not contribute to the conductivity. Therefore, the augment in defect associates also results in a lower leakage current. It is deserved to note that the incorporation of Y^{3+} into Al_2O_3 films can exert a great inhibiting effect on leakage current. Moreover, it can be reasonably deduced that the leakage current of aluminum oxide films can be effectively tuned by Y doping.

4 Analysis of dielectric breakdown

It is known that the weak-spot breakdown occurs before the intrinsic breakdown. The existence of defects will make significant influence on the dielectric strength. For better reliability of results, weibull distribution is used to take the analysis of breakdown voltage to predicate the reasonable value of breakdown voltage [25]. For comparison, the breakdown voltage has been converted into breakdown strength according to the formula of $E = U/d$, where U is voltage, d is thickness of films, E is electric strength. Figure 4 depicts the dielectric breakdown characteristics for Y doping aluminum oxide films, while the inserted figure shows the breakdown strength dependence of the Y doping content. As shown in Fig. 4, the breakdown strength of Y-doped aluminum oxide films is a litter lower than the pure aluminum oxide thin films, which means that Y doping has no positive influence on the breakdown strength.

The weakening effect of Y doping on breakdown strength of aluminum oxide films may be ascribed to the structure defects generated by the substitution of Al by Y atoms. The increasing defects greatly accelerate the occurrence of weak-spot breakdowns which are the destruction for films and thus decrease the dielectric strength of films. It is evident from the real time observation shown in Fig. 5 that reveals the occurrence of weak-spot breakdowns in advance. Generally speaking, there are three dielectric breakdown forms for dielectrics in MOS

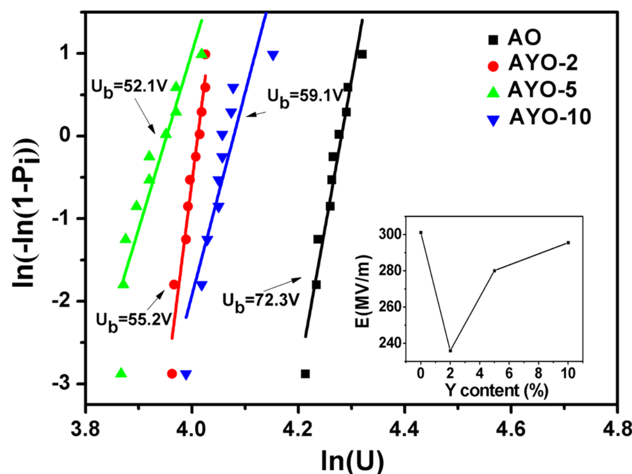

Fig. 4 Weibull distribution of the Breakdown Voltage of the $Al_{2-2x}Y_{2x}O_3$ thin films. Inset shows the dependence of breakdown strength on Yttrium molar fraction of the $Al_{2-2x}Y_{2x}O_3$ thin films (U is the breakdown voltage of each specimen, P_i is the cumulative failure probability, E is the average breakdown strength)

devices [26]. Likewise, we have also founded the same dielectric breakdown forms for alumina films in MIM structure, including single-hole breakdown, propagating breakdown and the maximum voltage breakdown. As illustrated in Fig. 5, Y doping improves the occurrence frequency of the first two kinds of breakdown events which decreases the final breakdown strength.

However, as the further increase of Y doping content, the dielectric strength increases. It is shown by the FTIR analysis that the content of hydroxyl and absorbed water decreases with the increasing of Y doping. And the existence of hydroxyl and absorbed water is harmful to the dielectric strength of films. In this way, the dielectric strength will gain some enhancement for the increasing of Y doping content. Moreover, we did the breakdown property test with different relative humidity at the same temperature. The variation of relative humidity changes the amount of water absorbed in films. By this way, we study and get to know the role of absorbed water on leakage current and breakdown behavior of aluminum oxide films. It is seen in Fig. 6 that the increase of relative humidity lead to a greater leakage current and smaller dielectric strength, which is further evidence that hydroxyl and absorbed water is harmful to the dielectric breakdown property.

Based on the above investigations, it can be concluded that the incorporation of Y^{3+} makes negative influence on dielectric breakdown properties. The reliability of Y-doped aluminum oxide films is somewhat lower than undoped aluminum oxide films in the case of dielectric strength. But in the Y-doped thin films, breakdown strength increases with the further Y doping. It is the result of two factors,

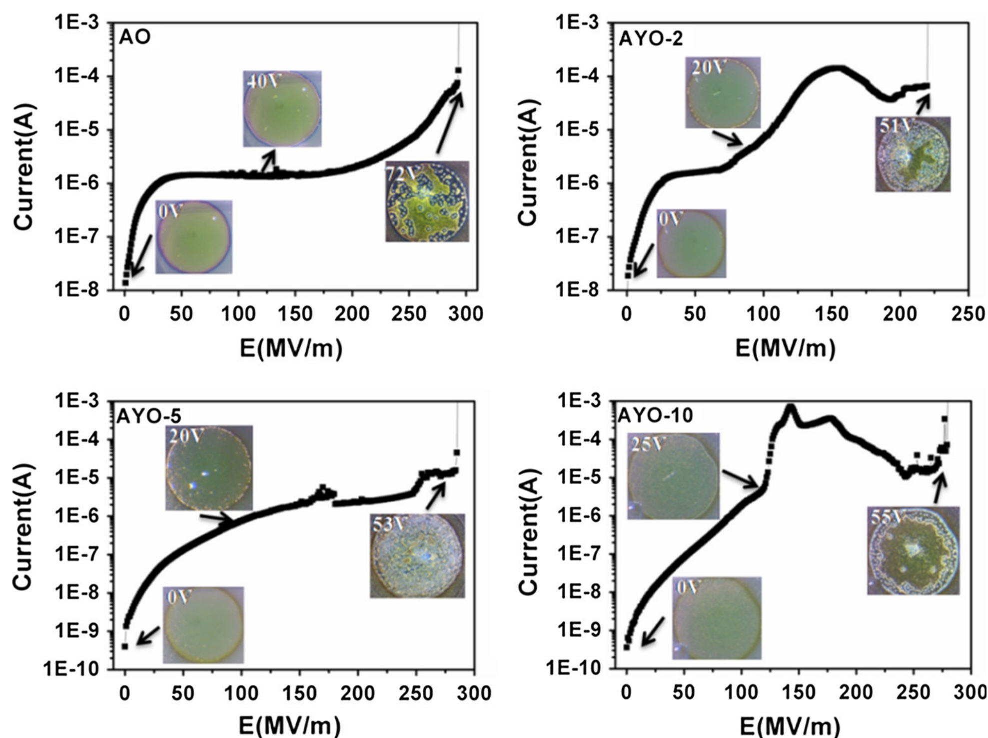

Fig. 5 The real time observation of the $Al_{2-2x}Y_{2x}O_3$ films during breakdown process recorded with a metallographic microscope

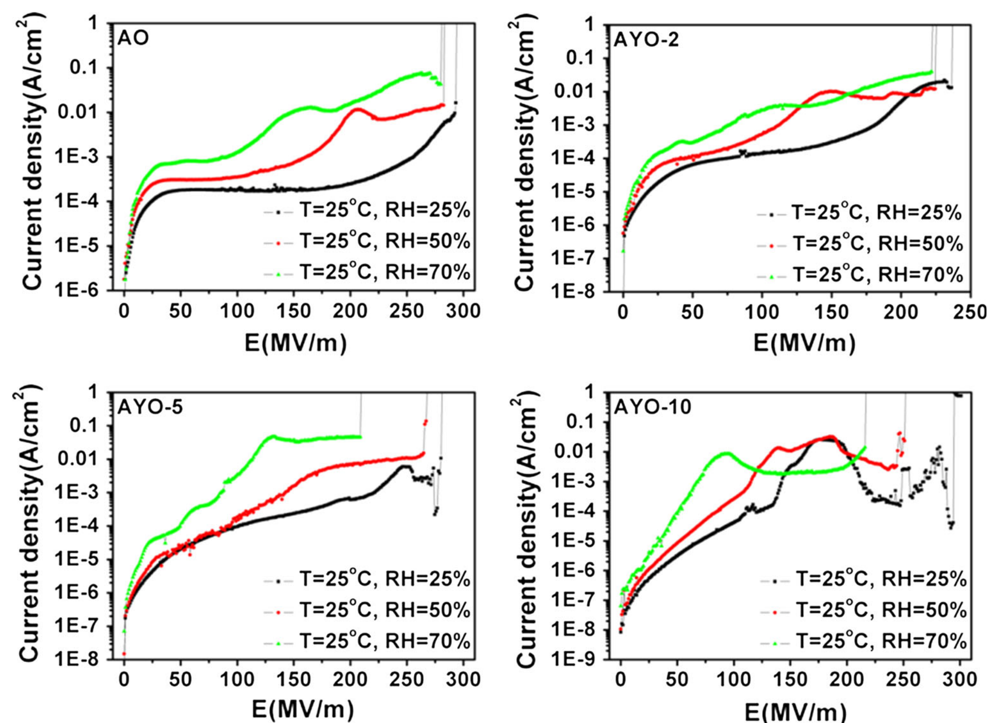

Fig. 6 Leakage current density–electric field characteristics of $Al_{2-2x}Y_{2x}O_3$ films measured with different relative humidity at room temperature

including defects caused by substitution of Al by Y and the effect of absorbed water. Therefore, the 10 mol% Y-doped Al_2O_3 film is a potential dielectric that can be expected to be used in many applications due to its lowest leakage current and high dielectric strength.

5 Analysis of dielectric constant and loss

Figure 7 shows the dielectric constant and dielectric loss changing with the frequency ranging from 20 Hz to 2 MHz. It is observed that the frequency dependence of

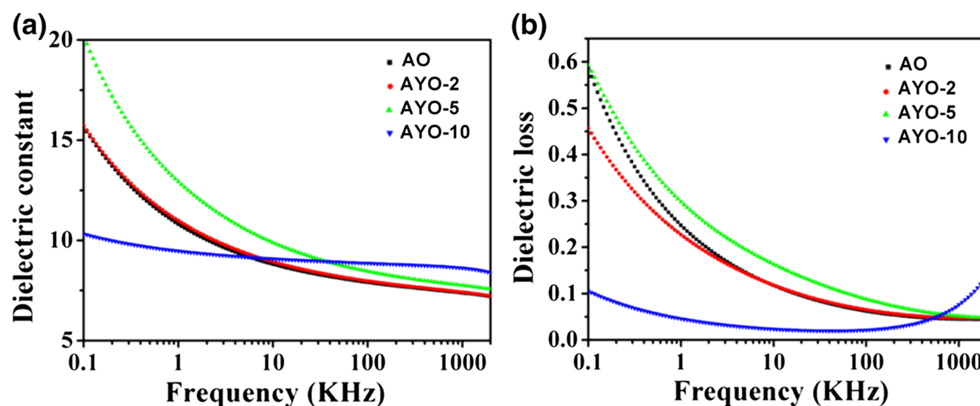

Fig. 7 **a** Frequency-dependent permittivity and **b** dielectric loss for $Al_{2-2x}Y_{2x}O_3$ thin films

both permittivity and dielectric loss can be divided into two different sub-regions. For frequencies above 10 kHz, the dielectric constant and dielectric loss remains almost frequency independent. However, for frequencies below 10 kHz a steep increase of the dielectric constant and loss factor is observed.

At the frequency of 1 MHz, dielectric constant and dielectric loss of $Al_{2-2x}Y_{2x}O_3$ films are between 7–8 and 0.05–0.07 respectively, the concrete values are not markedly different from each other. Therefore, Y doping do not make a remarkable difference on dielectric properties of aluminum oxide films at high frequencies.

According to dielectric relaxation, at low frequency, the dielectric constant and loss are associated with increased conduction losses [27, 28]. In addition, the dielectric constant increases with the increasing of dipoles polarization. Since conduction loss and dipoles polarization relate to the hydroxyl and absorbed water existing in films, which is in good agreement with the leakage current measurement, the decrease of the content of hydroxyl and absorbed water as increasing of Y doping may lead to the smallest dielectric constant and loss for 10 mol% Y-doped aluminum oxide films.

6 Conclusion

In conclusion, we have prepared amorphous $Al_{2-2x}Y_{2x}O_3$ thin films by sol–gel. The influence of Yttrium doping on leakage current and dielectric properties of aluminum oxide films has been studied. The substitution doping of Yttrium leads to a lower leakage current and then improves the reliability of aluminum oxide films. It should be noted that the leakage current of aluminum oxide films can be effectively tuned in right content of Y doping. However, in respect to dielectric strength, it is observed that Y doping is helpful to the breakdowns at defects or weak spots in the films and thus decreases the dielectric strength. But with the further increase of Y doing content, dielectric strength increases on account of the influence of absorbed water. So, in a nutshell, the 10 mol% Y-doped Al_2O_3 films is provided with the lowest leakage current and excellent dielectric properties. It is reasonable to deduce that substitution of Y into aluminum oxide films may be a promising way to enhance the reliability of dielectric films.

Acknowledgments This work is supported by the Ministry of Science and Technology of China through 973-project (Grant Number 2015CB654601), International Science and Technology Cooperation Program of China (Grant Number 2013DFR50470) and National Science Foundation of China (Grant Number 51272177).

References

1. E. Ciliberto, I. Fragala, R. Rizza, G. Spoto, G.C. Allen, Appl. Phys. Lett. **67**, 1624–1626 (1995)
2. J. Litvinov, Y.J. Wang, J. George, P. Chinwangso, S. Brankovic, R.C. Willson, D. Litvinov, Surf. Coat. Technol. **224**, 101–108 (2013)
3. K.H. Zaininger, A.S. Waxman, IEEE. T. Electron. Dev. **16**, 333–338 (1969)
4. K.P. Pande, V.K.R. Nair, D. Gutierrez, J. Appl. Phys. **54**, 5436–5440 (1983)
5. T.H. Hua, M. Armgarth, J. Electron. Mater. **16**, 27–31 (1987)
6. M. Ishida, I. Katakabe, T. Nakamura, N. Ohtake, Appl. Phys. Lett. **52**, 1326–1328 (1988)
7. K.B. Jinesh, J.L. Van Hemmen, M.C.M. Van De Sanden, F. Roozeboom, J.H. Klootwijk, W.F.A. Besling, W.M.M. Kessels, J. Electrochem. Soc. **158**, G21–G26 (2011)
8. M. Aguilar-Frutis, M. Garcia, C. Falcony, G. Plesch, S. Jimenez-Sandoval, Thin Solid Films **389**, 200–206 (2001)
9. J. Peng, Q. Sun, S. Wang, H. Wang, Appl. Phys. Lett. **103**, 061603 (2013)
10. G.W. Hyung, J. Park, J.R. Koo, Z. Li, S.J. Kwon, E.S. Cho, Y.K. Kim, Jpn. J. Appl. Phys. **51**, 025702 (2012)
11. E.P. Gusev, M. Copel, E. Cartier, I.J.R. Baumvol, C. Krug, M.A. Gribelyuk, Appl. Phys. Lett. **76**, 176–178 (2000)
12. J. Kolodzey, E.A. Chowdhury, T.N. Adam, G. Qui, I. Rau, J.O. Olowolafe, J.S. Suehle, Y. Chen, IEEE. T. Electron. Dev. **47**, 121–128 (2000)
13. W.H. Lee, J.T. Clemens, R.C. Keller, L. Manchanda, Tech. Dig. Symp. VLSI Technol. **1**, 117–118 (1997)
14. N.H. Fletcher, A.D. Hilton, B.W. Ricketts, J. Phys. D Appl. Phys. **29**, 253 (1996)

15. E.K. Michael, S. Trolier-McKinstry, J. Appl. Phys. **118**, 054101 (2015)
16. Q. Chen, Y. Wang, X. Zhou, Q.M. Zhang, S. Zhang, Appl. Phys. Lett. **92**, 142909 (2008)
17. X. Song, Y. Zhang, Y. Chen, Q. Zhang, J. Zhu, D. Yang, J. Electron. Mater. **44**, 4819–4824 (2015)
18. D.M. Smyth, *The Defect Chemistry of Oxides, ch. 5* (Oxford University Press, New York, 2000)
19. Y. Kono, N. Ohya, Y. Saiga, K. Suekuni, T. Takabatake, K. Akai, S. Yamamoto, J. Electron. Mater. **40**, 845–850 (2011)
20. F. Wang, Y. Han, C.S. Lim, Y. Lu, J. Wang, J. Xu, H. Chen, C. Zhang, M. Hong, X. Liu, Nature **463**, 1061–1065 (2010)
21. T. Maruyama, S. Arai, Appl. Phys. Lett. **60**, 322–323 (1992)
22. Y.T. Chu, J.B. Bates, C.W. White, G.C. Farlow, J. Appl. Phys. **64**, 3727–3730 (1988)
23. H.A. Al-Abadleh, V.H. Grassian, Langmuir **19**, 341–347 (2003)
24. G. Dearnaley, A.M. Stoneham, D.V. Morgan, Rep. Prog. Phys. **33**, 1129 (1970)
25. M. Yao, R. Xiao, Y. Peng, J. Chen, B. Hu, X. Yao, J. Sol-Gel, Sci. Technol. **74**, 39–44 (2015)
26. N. Klein, IEEE. Trans. Electron. Dev. **11**, 788–805 (1966)
27. A.K. Jonscher, J. Phys. D Appl. Phys. **32**(14), R57 (1999)
28. A.P. Kerasidou, P.K. Karahaliou, N.I. Xanthopoulos, P. Svarnas, IEEE. T. Dielect. El. In **21**, 230–235 (2014)